Research paper

An isomer-specific study of solid nitromethane decomposition pathways – Detection of aci-nitromethane (H$_2$CNO(OH)) and nitrosomethanol (HOCH$_2$NO) intermediates

Pavlo Maksyutenko [a,b], Marko Förstel [a,b], Parker Crandall [a,b], Bing-Jian Sun [c], Mei-Hung Wu [c], Agnes H.H. Chang [c,*], Ralf I. Kaiser [a,b,*]

[a] Department of Chemistry, University of Hawaii, 2545 McCarthy Mall, 96822 HI, USA
[b] W. M. Keck Research Laboratory in Astrochemistry, University of Hawaii, 2545 McCarthy Mall, 96822 HI, USA
[c] Department of Chemistry, National Dong Hwa University, Shoufeng, Hualien 974, Taiwan

A B S T R A C T

An isomer specific study of energetic electron exposed nitromethane ices was performed *via* photoionization – reflectron time of flight mass spectrometry (PI-ReTOF-MS) of the subliming products employing tunable vacuum ultraviolet light for ionization. Supported by electronic structure calculations, nitromethane (CH$_3$NO$_2$) was found to isomerize to methyl nitrite (CH$_3$ONO) and also *via* hydrogen migration to the hitherto elusive aci-nitromethane isomer (H$_2$CNO(OH)). The latter isomerizes to nitrosomethanol (HOCH$_2$NO) through hydroxyl group (OH) migration, and, probably, ring closure to the cyclic 2-hydroxy-oxaziridine isomer (c-H$_2$CON(OH)) as well. The importance of hydrogen migrations was also verified *via* the nitrosomethane (CH$_3$NO) – formaldehyde oxime isomer (CH$_2$NOH) pair.

© 2016 Elsevier B.V. All rights reserved.

1. Introduction

Due to the importance of nitromethane (CH$_3$NO$_2$) as a model explosive of nitrohydrocarbon-based (RNO$_2$) energetic materials [1] and monopropellants [2], there is a crucial prerequisite from the material science community to study the decomposition mechanisms of nitromethane along with the successive reactions of the carbon-, nitrogen-, and oxygen-centered radicals produced in this process [3]. In contrast to the condensed phase, the unimolecular decomposition of nitromethane in the gas phase has been extensively studied over the past decades *via* ultraviolet (UV) photolysis and infrared multi-photon dissociation (IRMPD) [4]. In the ultraviolet photolysis, the dominant channel is a barrierless dissociation to the methyl radical (•CH$_3$) and nitrogen dioxide (•NO$_2$), whereas in the case of IRMPD this pathway competes with a roaming-mediated nitromethane – methylnitrite (CH$_3$ONO) isomerization followed by decomposition to the methoxy radical (CH$_3$O•) plus nitrogen monoxide (•NO) and formaldehyde (H$_2$CO) plus nitrosylhydride (HNO) (Fig. 1) [5,6].

Until lately, only limited experiments have been carried out in the condensed phase. Matrix isolation studies employing ultraviolet photolysis combined with Fourier transform infrared (FTIR) detection [7,8] suggested that the nitromethane (CH$_3$NO$_2$) – methyl nitrite (CH$_3$ONO) isomerization represents the key step in the decomposition mechanism. A computational analysis proposed that an external electric field lowers the isomerization barrier, potentially providing a detonation stability control [9]. However, more exotic isomers have not received much attention. These are: aci-nitromethane (H$_2$CNO(OH)) **(3)**, 2-hydroxy-oxaziridine (c-H$_2$CON(OH)) **(4)**, nitrosomethanol (HOCH$_2$NO) **(5)**, and formohydroxamic acid (HCONH (OH), HOCHNOH) **(6/7)** (Table 1). What little is known on these isomers is summarized in the next paragraphs.

Nitrosomethanol (HOCH$_2$NO) **(5)** was first discovered by Mueller and Huber [13]. By exciting the S$_1$(nπ*) transition at 365 nm of matrix isolated methyl nitrite (CH$_3$ONO) **(2)**, a hydrogen-bonded formaldehyde (H$_2$CO) – nitrosylhydride (HNO) complex was formed. Photolysis of this complex produced either the *trans* (λ = 345 nm) or the *cis* (λ > 645 nm) isomer of nitrosomethanol (HOCH$_2$NO) **(5)**. Yu and Liu [14] explored the photochemical study by Mueller and Huber *via ab initio* methods and found that the photolysis of the above mentioned complex should produce *trans*-nitrosomethanol (HOCH$_2$NO) **(5)** exclusively, which can be further transformed into the *cis* form at λ > 645 nm. Kalkanis and Shields [15] predicted that nitrosomethanol
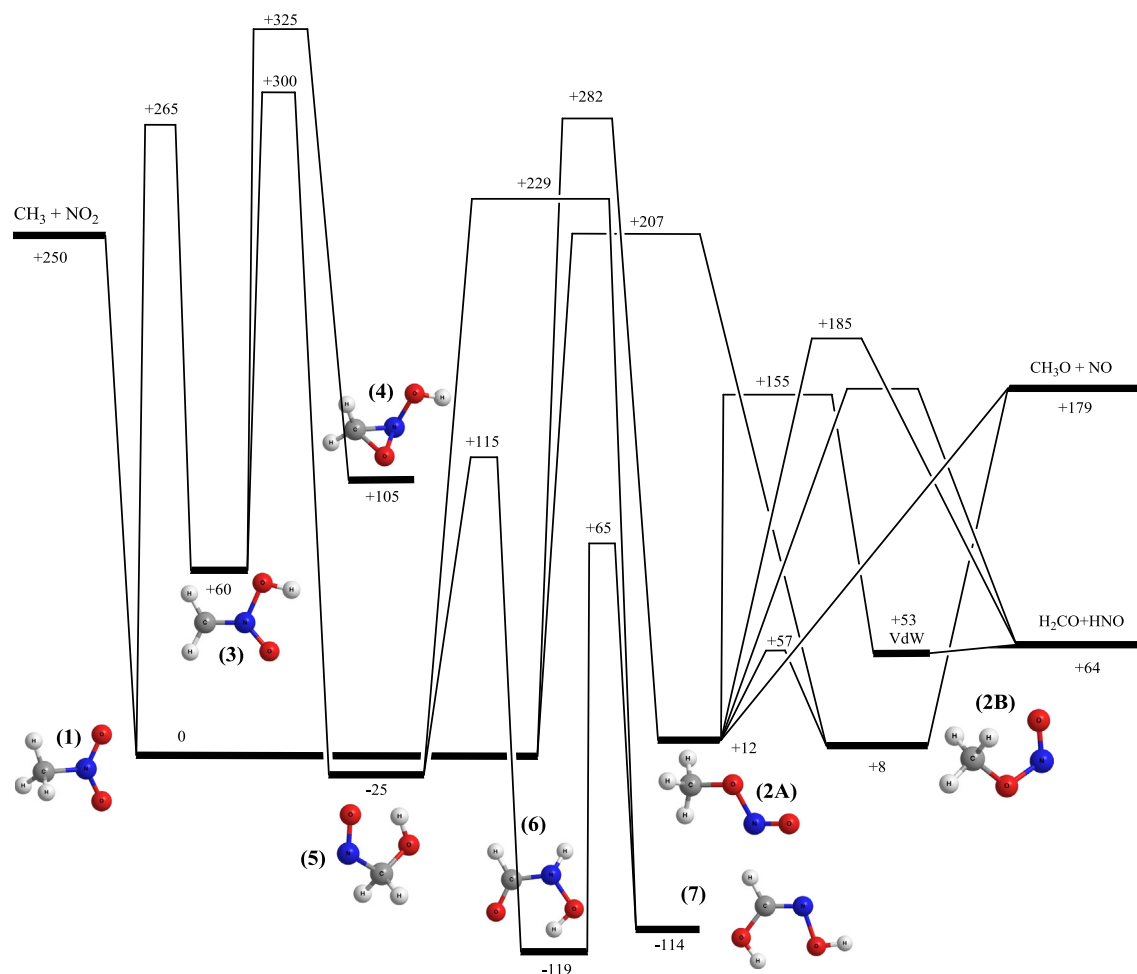
Fig. 1. Potential energy surface (PES) for nitromethane isomerization and decomposition pathways in the gas phase with energetics indicated relative to nitromethane (kJ mol^{-1}). The isomers are: (1) nitromethane, (2A) and (2B) *trans*- and *cis*-methyl nitrate, (3) aci-nitromethane, (4) 2-hydroxy-oxaziridine, (5) nitrosomethanol, (6 and 7) 1-Z and 2-Z formohydroxamic acid.

(HOCH$_2$NO) **(5)** was the dominant reaction product of the hydroxymethyl (CH$_2$OH) – nitrogen monoxide (NO) radical–radical recombination. The calculations were later improved to the MP4SDTQ/6-311+G(d,p) level with MP2(full)/6-31G(d,p) geometry optimization by Shin et al. [16].

The aci-nitromethane isomer (H$_2$CNO(OH)) **(3)** was proposed tentatively in the gas phase *via* neutralization–reionization mass spectrometry by Egsgaard et al. [17]. In the condensed phase, it was inferred as the initial reaction product in the protonation of the nitromethyl anion (H$_2$CNO$_2^-$) [18]. More recently, the calculations of Dhanya et al. [19] explained the appearance of the hydroxyl radical fragment (OH) in photolysis by an aci-nitromethane (H$_2$CNO(OH)) **(3)** intermediate. Sung et al. [20] applied a quantum mechanics/molecular mechanics approach to study nitrogen oxides reduction with acetic acid or acetaldehyde in the novel Barium Y zeolite, and identified aci-nitromethane (H$_2$CNO(OH)) **(3)** as one of the key intermediates. Further, Wang et al. [21] applied the ONIOM computational method to investigate nitromethane (CH$_3$NO$_2$) **(1)** confined inside armchair (5, 5) single-walled carbon nanotubes (CNT) to understand the confinement effect of CNT on the initial reactions of nitro-energetic compounds. They determined that the barrier for nitromethane (CH$_3$NO$_2$) **(1)** to aci-nitromethane (H$_2$CNO(OH)) **(3)** isomerization was decreased by the confinement effect from 260 to 239 kJ mol^{-1}, and that the barrier for nitromethane (CH$_3$NO$_2$) **(1)** to methyl nitrite (CH$_3$ONO) **(2)** rearrangement decreased from 272 to 193 kJ mol^{-1}.

A cyclic 2-hydroxy-oxaziridine isomer (c-H$_2$CON(OH)) **(4)** has never been observed experimentally, but was predicted to exist based on theoretical studies. The first comprehensive *ab initio* study of the CH$_3$NO$_2$ PES was performed by McKee in 1986 employing – by today's standards – a very modest MP2/6-31G* level of theory [22]. This work identified five structural isomers and defined their energetics and isomerization barriers. Hu et al. [23] extended the calculations to ten CH$_3$NO$_2$ isomers, 46 transition states, and 16 dissociation pathways. These results, obtained at the G2MP2// B3LYP/6-311++G(2d,2p) level of theory, qualitatively agree with those by McKee. The 2-hydroxy-oxaziridine isomer (c-H$_2$CON (OH)) **(4)** can be formed from aci-nitromethane (H$_2$CNO(OH)) **(3)** *via* a 229 kJ mol^{-1} barrier. It is 121 kJ mol^{-1} less stable than nitromethane (CH$_3$NO$_2$) **(1)**, but it resides in a deep potential energy minimum with barriers to isomerization into aci-nitromethane (H$_2$CNO (OH)) **(3)**, nitrosomethanol (HOCH$_2$NO) **(5)**, and formohydroxamic acid (HC(O)N(H)OH) **(6)** in excess of 190 kJ mol^{-1}. Most recently, Zhang et al. [24] studied the CH$_3$/NO$_x$ potential energy surfaces and addressed most of the known isomers, including 2-hydroxy-oxaziridine **(4)** (Table 2).

Finally, the formohydroxamic acid isomer (HCONHOH) **(6/7)** represents a well-studied compound of biological importance [25]. This molecule has also been considered for uranium extraction process [26]. Formohydroxamic acid can exist in keto and iminol forms. The isomer has been addressed computationally by Hu et al. [23] and Zhang et al. [24].

Table 1
Isomers of nitrosomethane (CH_3NO), nitromethane (CH_3NO_2), and of the nitromethane dimer (($CH_3NO_2)_2$) along with calculated and experimental ionization energies. Energies relative to the most stable isomer are listed in parentheses (kJ mol^{-1}).
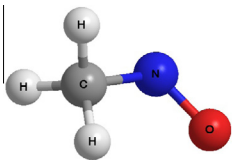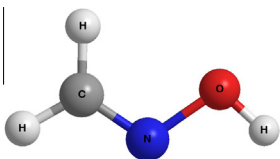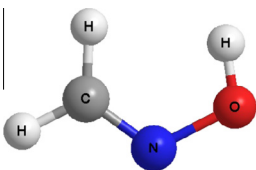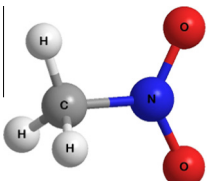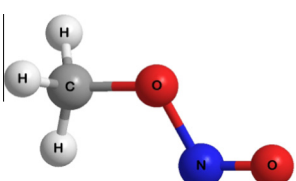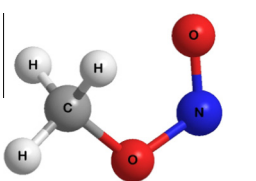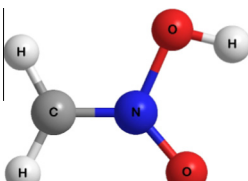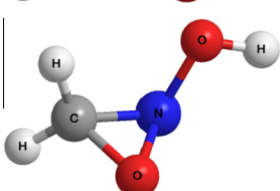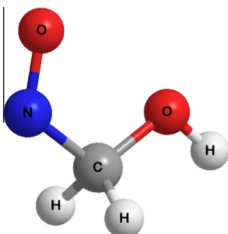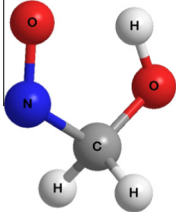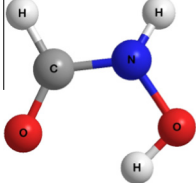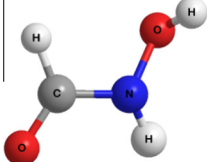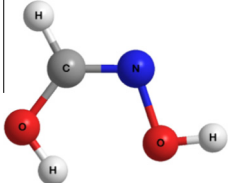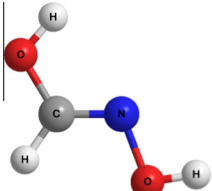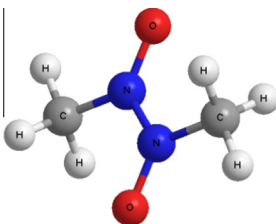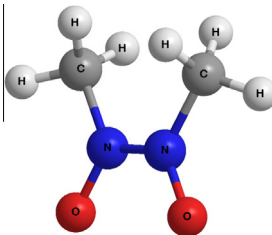
#	Name	Structure (B3LYP)	Ionization energy, eV			
			IE, eV (B3LYP//CCSD(T))/CBS	IE, eV (MP2//CCSD(T))	IE, eV (CCSD//CCSD(T))	Exp.
1	Nitrosomethane		9.25 (50.5)	9.18 (48.0)	9.07 (47.7)	9.3[10]
2A	*Trans*-Formaldehyde oxime		10.03 (0.0)	9.96 (0.0)	9.87 (0.0)	10.1[10]
2B	*Cis*-Formaldehyde oxime		9.83 (19.4)	9.77 (18.7)	9.67 (18.8)	
1	Nitromethane		11.10 (0.0)	10.96 (0.0)	10.88 (0.0)	11.08 [11]
2A	*Trans*-methyl nitrite		10.31 (11.5)	10.28 (2.6)	10.11 (3.9)	10.4[12]
2B	*Cis*-methyl nitrite		10.50 (7.6)	10.43 (−1.5)	10.31 (−0.01)	
3	Aci-nitromethane		9.57 (60.1)	9.38 (60.6)	9.32 (62.0)	
4	2-Hydroxy-oxaziridine		9.99 (104.7)	9.65 (115.6)	9.62 (117.3)	

Table 1 (continued)

#	Name	Structure (B3LYP)	Ionization energy, eV			
			IE, eV (B3LYP//CCSD(T))/CBS	IE, eV (MP2//CCSD(T))	IE, eV (CCSD//CCSD(T))	Exp.
5A	*Trans*-nitrosomethanol		8.77 (−10.6)	8.75 (−13.1)	8.50 (−11.9)	
5B	*Cis*-nitrosomethanol		8.90 (−24.9)	8.75 (−27.9)	8.63 (−26.7)	
6A	1-Z formohydroxamic acid		9.50 (−118.6)	9.40 (−116.0)	9.26 (−115.1)	
6B	1-E formohydroxamic acid		9.65 (−111.5)	9.59 (−111.6)	9.43 (−110.6)	
7A	2-Z formohydroxamic acid		9.66 (−113.9)	9.47 (−114.3)	9.44 (−112.9)	
7B	2-E formohydroxamic acid		9.42 (−97.8)	9.23 (−99.2)	9.21 (−97.9)	
1A	*Trans*-nitrosomethane dimer		8.38 (0.0)	8.20 (0.0)	8.12[a] (0.0)	8.3[10]

Table 1 (*continued*)

#	Name	Structure (B3LYP)	Ionization energy, eV			
			IE, eV (B3LYP//CCSD(T))/CBS	IE, eV (MP2//CCSD(T))	IE, eV (CCSD//CCSD(T))	Exp.
1B	*Cis*-nitrosomethane dimer		8.22 (42.6)	8.30 (47.2)	7.93[a] (46.9)	

[a] Geometry optimization by CCSD/cc-pVDZ.

This aforementioned compilation suggests that a study of the isomerization processes from nitromethane (CH_3NO_2) to its more exotic isomers in the condensed phase is still in its infancy. Considering spectral congestion, broadening, and matrix-specific shifts, the infrared spectra in matrix isolation experiments are difficult to interpret unambiguously. A recent alternative approach, involving electron paramagnetic resonance (EPR) spectroscopy, confirmed the presence of carbon centered (CH_3 and CH_2NO_2), oxygen centered (CH_3O) and nitrogen centered (NO and NO_2) radical intermediates in the 121 nm irradiated nitromethane ice [29]. In the present study, our approach relies on reflectron time-of-flight mass spectrometry employing single photon vacuum ultraviolet (VUV) ionization. An exposure of nitromethane (D3-nitromethane) ices to ionizing radiation in form of energetic electrons and photons (Lyman α; 10.2 eV) and subliming the newly formed molecules *via* temperature programmed desorption revealed that the decomposition pathways of nitromethane in the condensed phase is considerably more complex than in the gas phase under collisionless conditions [4,30,31]. Since the VUV light can be tuned, the subliming isomers can be differentiated according to their ionization energies (Table 1) [32,33]. In addition to ionization energy selectivity, the structural isomers are disconnected based on their distinct sublimation temperatures according to their polarity in the temperature programmed desorption process.

2. Experimental

The details of the experimental apparatus have been reported elsewhere [31]. Briefly, thin films of solid nitromethane (CH_3NO_2) were prepared in a contamination-free chamber at base pressures of a few 10^{-11} Torr. The films were deposited onto a 15.0×12.7 mm^2 silver mirror interfaced *via* indium foil to a cold finger cooled to 5.6 ± 0.1 K by a two-stage Gifford–McMahon cryocooler. Degassed nitromethane (CH_3NO_2, Aldrich, 99+ %) vapor was introduced into the main chamber at a background pressure of 4×10^{-8} Torr for 4 min through a glass capillary array placed at 30 mm distance from the silver wafer. The ice thickness was determined *in situ via* laser interferometry with a helium–neon 632.8 nm laser. Two periods of laser intensity temporal oscillations during ice deposition correspond to 455 ± 10 nm, based on an index of refraction of the ice of 1.39 ± 0.02 [4]. The chemical reactions were initiated within the ice by scanning a 5 keV electron beam at 15 nA current over a rectangular area within the sample of 1.0 ± 0.1 cm^2 for 60 min. Possible sputtering effects of the irradiation process were below the detection limit of our QMS spectrometer. In an earlier study it was shown that the irradiation induced heating was below a few 0.1 K at comparable conditions [34]. The electrons were implanted at 70° relative to the surface

Table 2

Compilation of relative energies of CH_3NO_2 isomers calculated in this work in comparison with previous literature results.

#	Name	This work	A	B	C	D	E	F
		kJ mol^{-1}						
1	Nitromethane	0	0	0	0	0	0	0
2A	*Trans*-methyl nitrite	12	11	12	12	7	8	24
2B	*Cis*-methyl nitrite	8	8	7	12	5	5	15
3	Aci-nitromethane	60	60			51	62	91
4	2-Hydroxy-oxaziridine	105	105			95	121	131
5A	*Trans*-nitrosomethanol	−11	−10					25
5B	*Cis*-nitrosomethanol	−25	−25			−32		7
6A	Formohydroxamic acid (1-Z)	−119				−130	−112	
6B	Formohydroxamic acid (1-E)	−112				−124	−106	
7A	Formohydroxamic acid (2-Z)	−114				−128	−82	
7B	Formohydroxamic acid (2-E)	−98				−112	−92	

This work: CCSD(T)/CBS; **A**: re-calculation of MC Lin 2009; **B**: MC Lin, 2009 UCCSD(T)/CBS [27]; **C**: JM Bowman, 2013, UCCSD(T)/CBS [28]; **D**: Zhang 2005, MC-QCISD/B3LYP [24]; **E**: Hu 2002, G2MP2/B3LYP [23]; **F**: McKee 1986, MP2/6-31G* [22].

normal of the silver wafer. The averaged penetration depth of the energetic electrons was calculated *via* Monte Carlo simulations (CASINO) [35] to be 370 ± 10 nm, which is less than the thickness of the deposited ices of 455 ± 10 nm. This relationship insures that the energetic electrons do not interact with the silver substrate. The dose deposited into the ice sample was determined on average to be 4.1 ± 0.4 eV per molecule. The temperature programed desorption (TPD) studies were conducted by heating the irradiated ices at a rate of 0.5 K min^{-1} to 300 K. The subliming molecules were mass-analyzed with a reflectron time-of-flight mass spectrometer coupled with pulsed vacuum ultraviolet (VUV) photoionization in separate experiments at five distinct wavelengths: 118.2 nm (10.49 eV) [4,30,31], 121.4 nm (10.21 eV), 126.5 nm (9.80 eV), 135.6 nm (9.14 eV), and 156.3 nm (7.93 eV). The rationale of selecting these particular wavelengths for isomer specific photoionization will be discussed in Section 4. The 10.49 eV photons were produced *via* non-resonant tripling of the third harmonic (355 nm, 350 mJ per pulse, 30 Hz) of a Nd:YAG laser fundamental in xenon pulsed jet. The remaining four VUV photon energies utilized in the present study were generated *via* two-photon resonance enhanced difference frequency mixing in either xenon or krypton pulsed jets [36,37]. An ultraviolet photon ω_1 and a visible photon ω_2 were generated by the two Nd:YAG pumped dye lasers systems with an additional frequency conversion stage for ω_1 generation. Table S1 in *Supplementary Material* summarizes the laser system parameters utilized for the

VUV generation; Fig. S1 in the *Supplementary Material* presents the pulse sequence to ensure the temporal overlap of the two laser pulses with a rare gas pulse along with the proper ReTOF data acquisition timing.

3. Computational approach

The isomerization pathways of nitromethane (CH_3NO_2) are investigated by *ab initio* electronic structure calculations. The optimized geometries and harmonic frequencies of the isomers (and their cations) and transition states are predicted by the hybrid density functional B3LYP [38–41] level of theory with the cc-pVTZ basis set. The coupled cluster [42–45] CCSD(T)/cc-pVDZ, CCSD(T)/cc-pVTZ, and CCSD(T)/cc-pVQZ energies of these species are further computed and extrapolated to completed basis set limits [46], CCSD(T)/CBS, with B3LYP/cc-pVTZ zero-point energy corrections. The relative energies are expected to have an accuracy within 8 kJ mol^{-1} [47]. The adiabatic ionization energies were then calculated by taking the energy difference between the ionic and the lowest lying neutral state. The GAUSSIAN09 program [48] was utilized in the electronic structure calculations. Previous computations at this level compared with experimentally derived ionization energies suggests that the ionization energies derived from the CCSD(T)/cc-pVTZ with B3LYP/cc-pVTZ zero-point energy correction method are lower by not more than 0.1 eV compared to the experimentally derived values [32,49,48,30,46,27,43,26,42]. This is also confirmed by a comparison of literature values of the ionization energies with our computationally predicted ionization energies at the B3LYP// CCSD(T)/CBS level of theory as compiled in Table 1.

4. Results and discussion

4.1. Computed isomerization pathways

The computed isomerization pathways are compiled in Fig. 1, whereas the predicted ionization energies and energetics of the isomers are presented in Tables 1 and 2, respectively. Starting with nitromethane (CH_3NO_2) **(1)**, two initial isomerization pathways were located. The first pathway involves the traditional isomerization to *cis*- or *trans*-methyl nitrite (CH_3ONO) **(2B, 2A)** via classical barriers located at 207 and 282 kJ mol^{-1} with respect to nitromethane. The *cis* and *trans* isomers can interconvert through a barrier of only about 45 kJ mol^{-1}. The second isomerization route from nitromethane involves a hydrogen atom migration from the carbon to the oxygen atom to form aci-nitromethane (H_2CNO (OH)) **(3)** through a barrier of 265 kJ mol^{-1}; this isomer was found to be 60 kJ mol^{-1} less stable than nitromethane. Aci-nitromethane **(3)** can undergo a ring closure by overcoming a 265 kJ mol^{-1} barrier to yield an energetically even less favorable 2-hydroxy-oxaziridine (c-H_2CON(OH)) **(4)** isomer. Alternatively, aci-nitromethane **(3)** isomerizes via hydroxyl (OH) group migration from the nitrogen to the carbon atom via a lower barrier (240 kJ mol^{-1}) to rearrange to *cis*-nitrosomethanol ($HOCH_2NO$) **(5)**; this isomer is more stable by 25 kJ mol^{-1} with respect to nitromethane (CH_3NO_2) **(1)**. Nitrosomethanol ($HOCH_2NO$) **(5)** can isomerize further to keto formohydroxamic ($HCONHOH$) acid **(6)** via a 140 kJ mol^{-1} barrier. This isomer can subsequently rearrange via hydrogen shift to iminol formohydroxamic acid ($HOCHNOH$) **(7)** passing a 184 kJ mol^{-1} barrier. Alternatively, nitrosomethanol ($HOCH_2NO$) **(5)** isomerizes to iminol formohydroxamic acid ($HOCHNOH$) **(7)** by overcoming a transition state located 254 kJ mol^{-1} above nitrosomethanol ($HOCH_2NO$) **(5)**.

4.2. Photoionization studies

The temperature programmed desorption studies exploiting PI-ReTOF-MS supplied a wealth of new information on the products escaping previous FTIR studies of this system [31] either because of the low concentration of the products or overlapping spectral features. On the other hand, the product detection with tunable energy of the ionizing photons allowed a discrimination between various isomers [31]. Fig. 2 represents an overview of the mass spectra (m/z) and how the ion counts at distinct m/z values depend on the temperature. These data were collected during the TPD process in separate experiments conducted with photon energies of 10.49 eV, 10.21 eV, 9.80 eV, 9.14 eV, and 7.93 eV. It is important to stress that at 7.93 eV, no signal was observed at all indicating that all products have ionization energies above this level. Our data interpretation focuses on the isomers of nitromethane (CH_3NO_2; m/z = 61) formed in the irradiation exposure along with possible decomposition products of these species via atomic oxygen loss leading to nitrosomethane isomers (CH_3NO; m/z = 45) and their dimers (($CH_3NO)_2$; m/z = 90) (Fig. 3). Smaller fragments connected to this study at m/z = 46, 31, and 30 were also analyzed (Fig. 4).

4.2.1. m/z = 90
The TPD profiles depicting strong sublimation events around 275 K (green) show similar pattern for photon energies between 10.49 eV and 9.14 eV. The signal is absent at 7.93 eV. These observations are consistent with our previous assignment [31] of m/z = 90 being the *cis*- and/or *trans*-nitrosomethane 'dimers' (($CH_3NO)_2$) holding ionization energies of 8.22 eV and 8.38 eV, respectively (Table 1). It further infers that a nitrosomethane monomer (CH_3NO) should be initially synthesized, from which the nitrosomethane dimer can be formed (Section 4.2.3). Nitrosomethane readily forms dimers because of the low barrier explained by a simultaneous formation of an N=N double bond and transformation of two N=O double to N—O single bonds, the two processes cancelling each other energetically. It has been reported that nitrosomethane preferentially forms the *cis* form of nitrosomethane dimer [50].

4.2.2. m/z = 61
The ionized species at m/z = 61 are observable from ionization energies between 10.49 eV and 9.14 eV (Fig. 3). Considering the computed ionization energies (Table 1), we conclude that the only possible isomers subliming in a broad region around 250 K (red) could be *cis*- and/or *trans*-nitrosomethanol ($HOCH_2NO$, IE = 8.90 and 8.77 eV, respectively). The fact that the lower temperature part of this part of the TPD profile grows faster with increasing detection photon energy then the higher temperature side suggests that either we observe here at least two distinct species with different photoionization efficiency curves with ionization energies below 9.14 eV, or that there is an additional contribution from a species with an ionization energy between 9.14 and 9.80 eV. The former case is consistent with the observation of both *cis*- and *trans*-nitrosomethanol **(5)**. A close look at the computed potential energy surface (Fig. 1) reveals that nitrosomethanol ($HOCH_2NO$) **(5)** can only be formed via isomerization of aci-nitromethane (CH_2NOOH) **(3)** (IE = 9.57 eV) or formohydroxamic acid isomer ($HCONHOH$) **(6/7)** (IE = 9.42–9.66 eV).

The sublimation event at 185 K (green) disappears at a photoionization energy of 9.14 eV. There are several isomers with ionization energy between 9.14 eV and 9.80 eV: aci-nitromethane (CH_2NOOH, **(3)**, IE = 9.57 eV) and formohydroxamic acid ($HCONHOH$, **(6/7)**, IE = 9.42–9.66 eV). A comparison of any of those structures with the nitromethane reactants and the underlying potential energy surface (Fig. 1) suggests the involvement of at
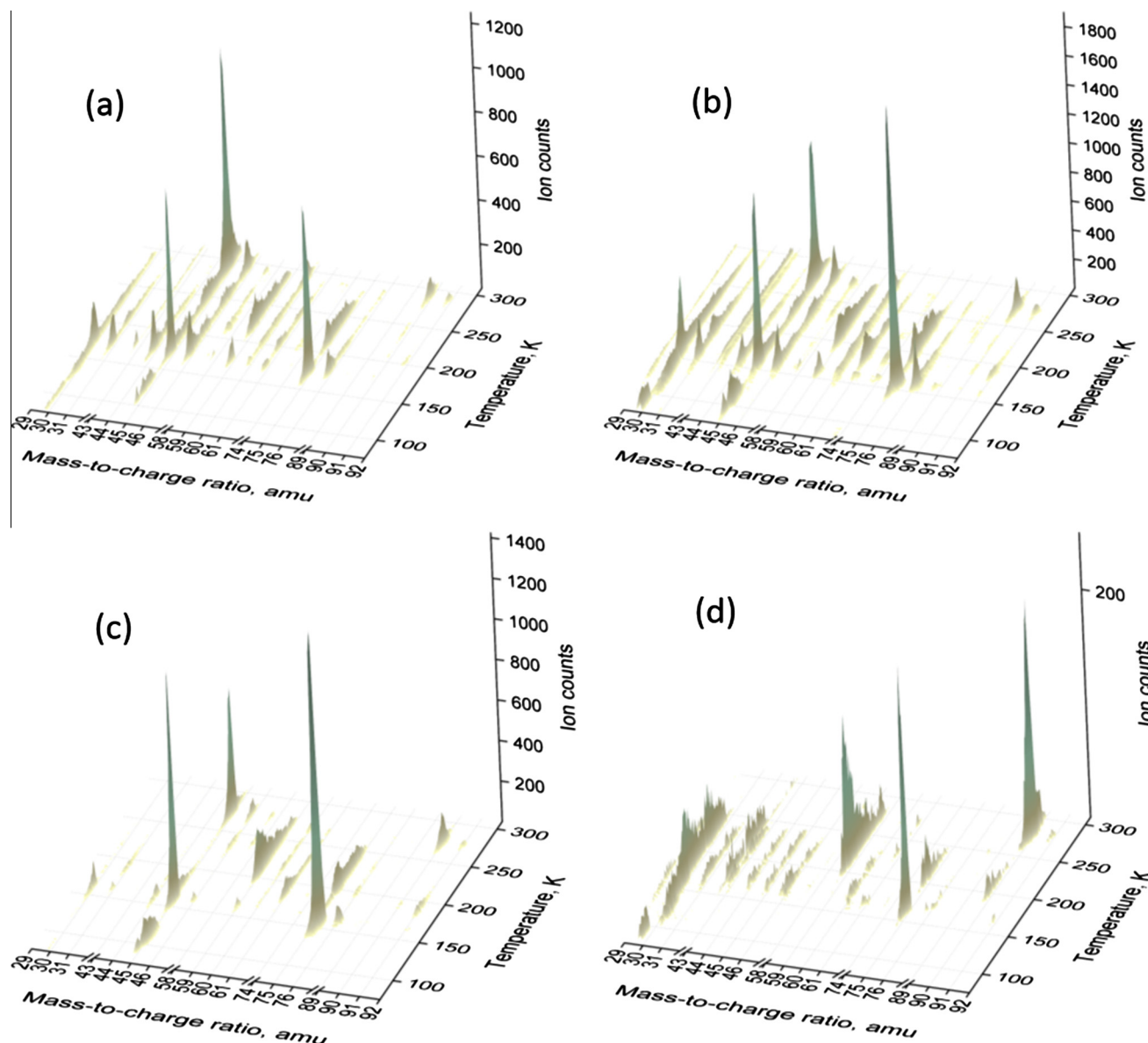
Fig. 2. PI-ReTOF-MS data of the newly formed products subliming into the gas phase from the irradiated nitromethane (CH_3NO_2) ice as a function of temperature at four different energies of the ionizing photon: (a) 10.49 eV, (b) 10.21 eV, (c) 9.80 eV, and (d) 9.14 eV.

least one hydrogen migration either from nitromethane (CH_3NO_2) (1) to aci-nitromethane (CH_2NOOH) (3) or from nitrosomethanol ($HOCH_2NO$) (5) to iminol formohydroxamic acid (HOCHNOH) (6/7). Since nitrosomethanol itself can only be formed *via* hydrogen migration from aci-nitromethane (CH_2NOOH) (3), these findings suggest that aci-nitromethane (CH_2NOOH) (3) must contribute to the sublimation profile at 185 K with possible contributions from formohydroxamic acid. Note that the absence of the 185 K peak in previous electron irradiation studies of D3-nitromethane with 10.49 eV photoionization detection at $m/z = 64$ [31] suggests a strong isotope effect in the hydrogen versus deuterium migration, effectively reducing the isomerization *via* deuterium shift below our detection limit.

Finally, a desorption feature at 160 K (yellow bar), is observable in the 9.14 eV profile as well. However, a control experiment that was conducted without exposure of the ice to energetic electrons (blank experiment) revealed a similar peak at 160 K. Since the nitromethane ionization energy (IE = 11.10 eV) is higher than the energy of the detection photons, we could only explain the

appearance of this ion in the blank experiment by a consecutive absorption of a second photon facilitated by high gas phase concentration of desorbing molecules during the peak sublimation event of the ice samples at a pressure of $\sim 10^{-9}$ Torr. Therefore, the real onset of the 160 K peak is at 9.80 eV, as for the 185 K signal. Therefore we cannot exclude a contribution of aci-nitromethane to this peak either. However, the ratio of signal at 185 K and 160 K increases with rising photoionization energy. We attribute the sharp increase from 10.21 to 10.49 eV mainly to *cis*- or *trans*-methylnitrite (*cis*- or *trans*-CH_3ONO; IE = 10.50 eV and 10.31 eV, respectively). The assignment of *cis*-methylnitrite *via* PI-ReTOF-MS also correlates with our recent infrared spectroscopic detection of this isomer [31]. Considering that ion counts increase by switching from 9.80 eV to 10.21 eV, these additional ion counts could be attributed to an isomer holding an ionization energy between 10.21 eV and 9.80 eV: the cyclic 2-hydroxy-oxaziridine isomer (c-$H_2CON(OH)$; IE = 9.99 eV). Alternatively, formohydroxamic acid isomers could be the major desorbing species at 160 K, displaying photoionization efficiency behavior
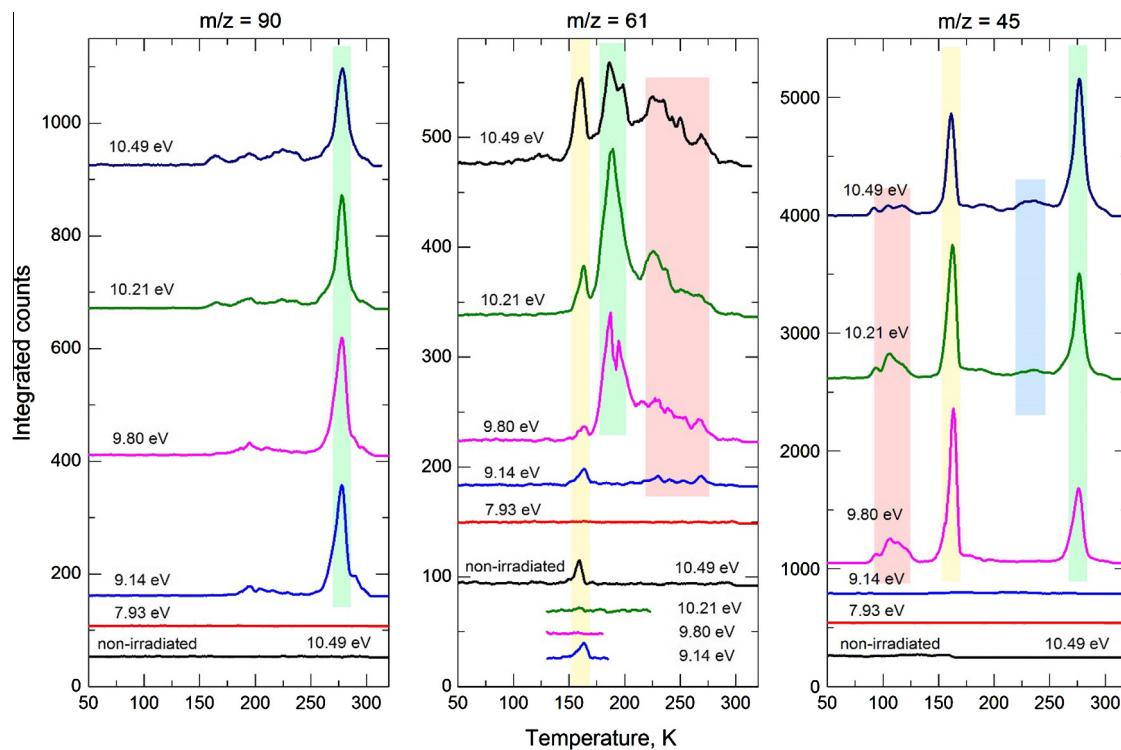
Fig. 3. Temperature programmed desorption (TPD) profiles of ionized products at $m/z = 90$ (left), $m/z = 61$ (center) and $m/z = 45$ (right) formed in electron irradiated nitromethane ice. The energies of the ionizing photons were, from top to bottom: (1) 10.49 eV, (2) 10.21 eV, (3) 9.80 eV, (4) 9.14 eV and (5) 7.93 eV. The bottom profiles of the TPD profiles of $m/z = 61$ correspond to blank experiments of the subliming non-irradiated ices and photoionizing the subliming species at 10.49 eV, 10.2 eV, 9.8 eV, and 9.15 eV.

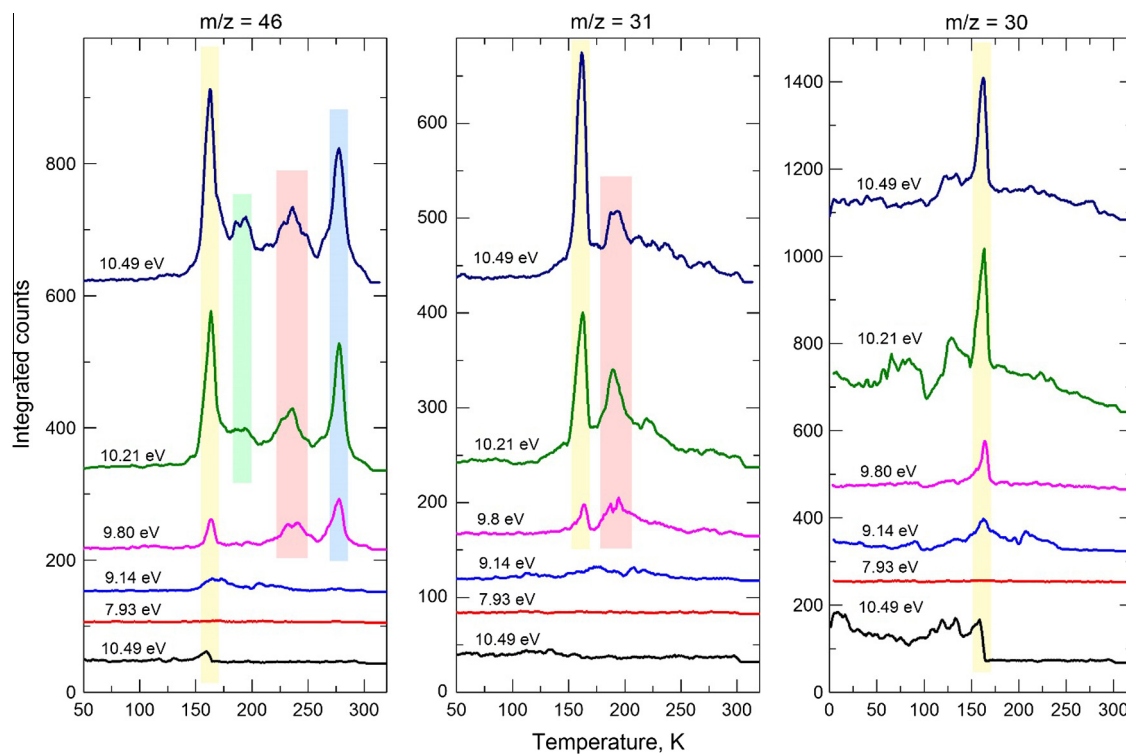**Fig. 4.** Temperature programmed desorption profiles of ionized products at $m/z = 46$ (left), $m/z = 31$ (center) and $m/z = 30$ (right) formed in electron irradiated nitromethane ice. The energies of the ionizing photons were, from top to bottom: (1) 10.49 eV, (2) 10.21 eV, (3) 9.80 eV, (4) 9.14 eV and (5) 7.93 eV. The bottom profiles correspond to non-irradiated ice at 10.49 eV detection photon energy.

that is different from aci-nitromethane (CH_2NOOH) **(3)**, which is the main contributor of the 185 K desorption event.

4.2.3. m/z = 45

Based on the detection of $m/z = 90$ and the assignment of the *cis-* and/or *trans*-nitrosomethane dimer, we also searched for the nitrosomethane monomer at $m/z = 45$. Here, two sublimation events emerged with high intensity maxima at around 160 K (yellow) and 275 K (green); two broader sublimation events are observable at around 110 K (red) and 230 K (blue). These events revealed an interesting pattern. *First*, the sublimation event at 275 K (green) overlaps with the sublimation profile recorded at $m/z = 90$ of the nitrosomethane dimer (($CH_3NO)_2$) (green). Therefore, signal at $m/z = 45$ of this sublimation event can be linked to the photofragment of the nitrosomethane dimer: nitrosomethane (CH_3NO). *Second*, considering the ionization energy of nitrosomethane of 9.25 eV and the computed ionization energies of the *cis-* and *trans*-formaldehyde oxime isomers (CH_2NOH) of 9.83 eV and 10.03 eV, the main product contributing to signal at $m/z = 45$ at the sublimation events peaking at 110 K and 160 K should be nitrosomethane (CH_3NO, IE = 9.25 eV). *Third*, the faint, broad feature around 230 K (blue) disappears at 9.80 eV. Considering the computed ionization energies, this signal can be assigned as *trans*-formaldehyde oxime (*trans*-CH_2NOH, IE = 10.03 eV), which is less stable by about 50 kJ mol^{-1} compared to nitrosomethane and likely formed by a keto-enol-type tautomerization *via* hydrogen shift from the carbon atom to the oxygen atom of the nitroso group of nitrosomethane. We have no explicit evidence of the formation of the *cis*-formaldehyde oxime (*cis*-CH_2NOH, IE = 9.83 eV). However, since this isomer ranges in stability between the detected nitrosomethane and *trans*-formaldehyde oxime (*trans*-CH_2NOH), its formation seems feasible. Since the relative intensities of the sublimation events peaking at 110 K (red) and 160 K (yellow) are changing from 10.49 eV to 9.80 eV, in particular the fine structure of the 110 K (red) sublimation event, the *cis*-formaldehyde oxime (*cis*-CH_2NOH) might contribute to ion counts around 110 K.

4.2.4. m/z = 46

The sublimation events at 160 K (yellow), 235 K (red) and 275 K (blue) are observed down to ionization energies of 9.80 eV and disappear at 9.14 eV. This is consistent with the assignment as nitrogen dioxide (NO_2) which has an ionization energy of 9.59 eV. This conclusion is in agreement with a recent EPR study of 121 nm irradiated nitromethane ice [29]. The species desorbing around 190 K (green) has an ionization energy between 9.80 eV and 10.21 eV. The species with general formulae H_2N_2O and CH_2O_2 are 46 amu, but their ionization energy values are not reported (except formic acid (HCOOH; IE = 11.3 eV)), precluding us from making further conclusions.

4.2.5. m/z = 31

The sharp desorption feature at 160 K (yellow) and the broader one at 190 K (red) are present down to photoionization energies of 9.80 eV. Furthermore, the ratio of the peak intensities changes, suggesting that, apart from nitrosyl hydride (HNO, IE = 10.1 eV), there should be at least one additional product with an ionization energy between 9.14 eV and 9.80 eV. Methylamine (CH_3NH_2) with an ionization energy of 9.6 eV would be a feasible candidate, but this would require multiple hydrogenation steps of nitrosomethane (CH_3NO) accompanied by formation of water (H_2O).

4.2.6. m/z = 30

The sharp desorption feature at 160 K (yellow) is visible at photoionization energies between 10.49 eV and 9.80 eV. This is consistent with the nitrogen monoxide (NO) assignment (IE = 9.26 eV).

5. Summary

The present study exploited an isomer specific detection of products generated in electron exposed nitromethane ices by probing the subliming products *via* photo ionization – reflectron time of flight mass spectrometry (PI-ReTOF-MS) of the subliming products ionized *via* a tunable vacuum ultraviolet light. Supported by electronic structure calculations, nitromethane (CH_3NO_2) **(1)** was found to isomerize to *cis*-methyl nitrite (CH_3ONO) **(2)** as detected previously *via* its 1615 cm^{-1} fundamental [31] and also *via* hydrogen migration to the hitherto elusive aci-nitromethane isomer (H_2CNO (OH)) **(3)**. These pathways require at least 207 kJ mol^{-1} and 265 kJ mol^{-1}, respectively. To the best of our knowledge, this is the first experimental detection of aci-nitromethane formed in the condensed phase. The aci-nitromethane isomer then undergoes hydroxyl (OH) migration to (HOCH$_2$NO) **(5)** *via* a barrier of about 240 kJ mol^{-1} as supplied by the impinging electrons. The importance of carbon–nitrogen hydrogen shifts in electron-irradiated nitromethane ices was also verified *via* the detection of the nitrosomethane (CH_3NO) – formaldehyde oxime isomer (CH_2NOH) pair. These studies suggest that in the condensed phase, hydrogen shifts are crucial reaction mechanisms, which are absent in the gas phase.

Acknowledgements

Appendix A. Supplementary material

Supplementary data associated with this article can be found, in the online version, at http://dx.doi.org/10.1016/j.cplett.2016.06.006.

References

[1] V. Bouyer, I. Darbord, P. Herve, G. Baudin, C. Le Gallic, F. Clement, G. Chavent, Shock-to-detonation transition of nitromethane: time-resolved emission spectroscopy measurements, Combust. Flame 144 (2006) 139–150.

[2] E. Boyer, K.K. Kuo, Modeling of nitromethane flame structure and burning behavior, Proc. Combust. Inst. 31 (2007) 2045–2053.

[3] N. Rom, S.V. Zybin, A.C.T. van Duin, W.A. Goddard, Y. Zeiri, G. Katz, R. Kosloff, Density-dependent liquid nitromethane decomposition: molecular dynamics simulations based on ReaxFF, J. Phys. Chem. A 115 (2011) 10181–10202.

[4] P. Maksyutenko, L.G. Muzangwa, B.M. Jones, R.I. Kaiser, Lyman [small alpha] photolysis of solid nitromethane (CH_3NO_2) and D3-nitromethane (CD_3NO_2) – untangling the reaction mechanisms involved in the decomposition of model energetic materials, Phys. Chem. Chem. Phys. 17 (2015) 7514–7527.

[5] R. Fernando, N.M. Ariyasingha, A.G. Suits, Imaging NO elimination in the infrared multiphoton dissociation of nitroalkanes and alkyl nitrites, Chem. Phys. Lett. 645 (2016) 76–83.

[6] A. Dey, R. Fernando, C. Abeysekera, Z. Homayoon, J.M. Bowman, A.G. Suits, Photodissociation dynamics of nitromethane and methyl nitrite by infrared multiphoton dissociation imaging with quasiclassical trajectory calculations: signatures of the roaming pathway, J. Chem. Phys. 140 (2014) 054305.

[7] H.W. Brown, G.C. Pimentel, Photolysis of nitromethane and of methyl nitrite in an argon matrix; infrared detection of nitroxy, HNO, J. Chem. Phys. 29 (1958) 883–888.

[8] M.E. Jacox, Photodecomposition of nitromethane trapped in solid argon, J. Phys. Chem. 88 (1984) 3373–3379.

[9] D.-L. Cao, W.-J. Shi, M. You, M. Li, A theoretical prediction of the possible trigger linkage of CH_3NO_2 and NH_2NO_2 in an external electric field, J. Mol. Model. 21 (2015) 1–9.

[10] D.C. Frost, W.M. Lau, C.A. McDowell, N.P.C. Westwood, A study by helium (He I) photoelectron spectroscopy of monomeric nitrosomethane, the cis and trans dimers, and formaldoxime, J. Phys. Chem. 86 (1982) 3577–3581.

[11] L. Paša-Tolić, K. Klasinc, S.P. McGlynn, The HeI PE spectrum and electronic structure of nitroethene, Chem. Phys. Lett. 170 (1990) 113–116.

[12] J.P. Gilman, T. Hsieh, G.G. Meisels, The unimolecular decomposition rates of energy selected methylnitrite and deuterated methylnitrite ions, J. Chem. Phys. 78 (1983) 3767–3773.

[13] R.P. Mueller, J.R. Huber, Reversible, light-induced isomerization of matrix-isolated molecules. Nitrosomethanol, J. Phys. Chem. 87 (1983) 2460–2462.

[14] J. Yu, R. Liu, Ab initio and CI studies on mechanism and reaction path of the photochemical reaction for the formation of nitrosomethanol, Acta Phys. Chim. Sin. 5 (1989) 340–347.

[15] G.H. Kalkanis, G.C. Shields, AM1 and PM3 calculations of the potential energy surfaces for hydroxymethyl radical reactions with nitric oxide and nitrogen dioxide, J. Phys. Chem. 95 (1991) 5085–5089.

[16] D. Shin, D. Koh, K. Kim, I. Hamilton, Insight into the chemical reaction of CH_2OH with NO: formation of N-hydroxy formamide as an isocyanic acid precursor, Catal. Today 119 (2007) 209–212.

[17] H. Egsgaard, L. Carlsen, H. Florêncio, T. Drewello, H. Schwarz, Aci-nitromethane—generated and characterized by neutralization reionization mass spectrometry, Ber. Bunsenges. Phys. Chem. 93 (1989) 76–80.

[18] J.N. Murrell, B. Vidal, M.F. Guest, Structure and electronic properties of the nitromethyl anion, nitromethane and aci-nitromethane, J. Chem. Soc., Faraday Trans. 2: Mol. Chem. Phys. 71 (1975) 1577–1582.

[19] S. Sengupta, Y. Indulkar, A. Kumar, S. Dhanya, P.D. Naik, P.N. Bajaj, Photodissociation dynamics of 2-nitropropane and 2-methyl-2-nitropropane at 248 and 193 nm, J. Phys. Chem. A 112 (2008) 12572–12581.

[20] C.-Y. Sung, L.J. Broadbelt, R.Q. Snurr, QM/MM study of the effect of local environment on dissociative adsorption in BaY zeolites, J. Phys. Chem. C 113 (2009) 15643–15651.

[21] L. Wang, C. Yi, H. Zou, J. Xu, W. Xu, Rearrangement and thermal decomposition of nitromethane confined inside an armchair (5, 5) single-walled carbon nanotube, Chem. Phys. 367 (2010) 120–126.

[22] M.L. McKee, Ab initio study of rearrangements on the nitromethane potential energy surface, J. Am. Chem. Soc. 108 (1986) 5784–5792.

[23] W.-F. Hu, T.-J. He, D.-M. Chen, F.-C. Liu, Theoretical study of the CH_3NO_2 unimolecular decomposition potential energy surface, J. Phys. Chem. A 106 (2002) 7294–7303.

[24] J.-X. Zhang, J.-Y. Liu, Z.-S. Li, C.-C. Sun, Theoretical study on the reaction mechanism of the methyl radical with nitrogen oxides, J. Comput. Chem. 26 (2005) 807–817.

[25] A.G. Guruge, D.P. Dissanayake, Ab initio study on transition states of formohydroxamic acid tautomerization in the presence of water molecules, Comput. Theor. Chem. 1032 (2014) 50–55.

[26] F.F. Fondeur, T.S. Rudisill, Thermal stability of formohydroxamic acid, Sep. Sci. Technol. 47 (2012) 2038–2043.

[27] R.S. Zhu, M.C. Lin, CH_3NO_2 decomposition/isomerization mechanism and product branching ratios: an ab initio chemical kinetic study, Chem. Phys. Lett. 478 (2009) 11–16.

[28] Z. Homayoon, J.M. Bowman, Quasiclassical trajectory study of CH_3NO_2 decomposition via roaming mediated isomerization using a global potential energy surface, J. Phys. Chem. A 117 (2013) 11665–11672.

[29] Y.A. Tsegaw, W. Sander, R.I. Kaiser, Electron paramagnetic resonance spectroscopic study on nonequilibrium reaction pathways in the photolysis of solid nitromethane (CH_3NO_2) and D3-nitromethane (CD_3NO_2), J. Phys. Chem. A 120 (2016) 1577–1587.

[30] R.I. Kaiser, P. Maksyutenko, A mechanistical study on non-equilibrium reaction pathways in solid nitromethane (CH_3NO_2) and D3-nitromethane (CD_3NO_2) upon interaction with ionizing radiation, Chem. Phys. Lett. 631 (2015) 59–65.

[31] R.I. Kaiser, P. Maksyutenko, Novel reaction pathways involved in the electron induced decomposition of solid nitromethane (CH_3NO_2) and D3-nitromethane (CD_3NO_2), J. Phys. Chem. C (2015).

[32] O. Kostko, J. Zhou, B.J. Sun, J.S. Lie, A.H. Chang, R.I. Kaiser, M. Ahmed, Determination of Ionization Energies of CnN (n = 4–12): vacuum ultraviolet

[33] F. Zhang, R.I. Kaiser, V.V. Kislov, A.M. Mebel, A. Golan, M. Ahmed, A VUV photoionization study of the formation of the indene molecule and its isomers, J. Phys. Chem. Lett. 2 (2011) 1731–1735.

[34] R.I. Kaiser, MeV-Ionen induzierte chemische Reaktionen in festem Methan, Ethen und Ethin. Theoretische und experimentelle Studien zur Wechselwirkung kosmischer Strahlung mit extraterrestrischen Eiskörpern., Berichte des Forschungszentrum Juelich, Report Juelich 2856, 1994, p. 143.

[35] D. Drouin, A.R. Couture, D. Joly, X. Tastet, V. Aimez, R. Gauvin, CASINO V2. 42—a fast and easy-to-use modeling tool for scanning electron microscopy and microanalysis users, Scanning 29 (2007) 92–101.

[36] R. Hilbig, G. Hilber, A. Lago, B. Wolff, R. Wallenstein, Tunable coherent VUV radiation generated by nonlinear optical frequency conversion in gases, in: P. Yeh (Ed.), Nonlinear Optics and Applications, 1986.

[37] J.W. Hepburn, Laser Techniques in Chemistry, Wiley, New York, NY, 1994.

[38] A.D. Becke, Density-functional thermochemistry. III. The role of exact exchange, J. Chem. Phys. 98 (1993) 5648–5652.

[39] A.D. Becke, Density-functional thermochemistry. II. The effect of the Perdew–Wang generalized-gradient correlation correction, J. Chem. Phys. 97 (1992) 9173–9177.

[40] A.D. Becke, Density-functional thermochemistry. I. The effect of the exchange-only gradient correction, J. Chem. Phys. 96 (1992) 2155–2160.

[41] C. Lee, W. Yang, R.G. Parr, Development of the Colle–Salvetti correlation-energy formula into a functional of the electron density, Phys. Rev. B 37 (1988) 785.

[42] G.D. Purvis III, R.J. Bartlett, A full coupled-cluster singles and doubles model: the inclusion of disconnected triples, J. Chem. Phys. 76 (1982) 1910–1918.

[43] C. Hampel, K.A. Peterson, H.-J. Werner, A comparison of the efficiency and accuracy of the quadratic configuration interaction (QCISD), coupled cluster (CCSD), and Brueckner coupled cluster (BCCD) methods, Chem. Phys. Lett. 190 (1992) 1–12.

[44] P.J. Knowles, C. Hampel, H.J. Werner, Coupled cluster theory for high spin, open shell reference wave functions, J. Chem. Phys. 99 (1993) 5219–5227.

[45] M.J. Deegan, P.J. Knowles, Perturbative corrections to account for triple excitations in closed and open shell coupled cluster theories, Chem. Phys. Lett. 227 (1994) 321–326.

[46] K.A. Peterson, D.E. Woon, T.H. Dunning Jr., Benchmark calculations with correlated molecular wave functions. IV. The classical barrier height of the H + H2 → H2 + H reaction, J. Chem. Phys. 100 (1994) 7410–7415.

[47] K.A. Peterson, T.H. Dunning Jr., Intrinsic errors in several ab initio methods: the dissociation energy of N2, J. Phys. Chem. 99 (1995) 3898–3901.

[48] M.J. Frisch, G.W. Trucks, H.B. Schlegel, G.E. Scuseria, M.A. Robb, J.R. Cheeseman, G. Scalmani, V. Barone, B. Mennucci, G.A. Petersson, H. Nakatsuji, M. Caricato, X. Li, H.P. Hratchian, A.F. Izmaylov, J. Bloino, G. Zheng, J.L. Sonnenberg, M. Hada, M. Ehara, K. Toyota, R. Fukuda, J. Hasegawa, M. Ishida, T. Nakajima, Y. Honda, O. Kitao, H. Nakai, T. Vreven, J.A. Montgomery Jr., J.E. Peralta, F. Ogliaro, M.J. Bearpark, J. Heyd, E.N. Brothers, K.N. Kudin, V.N. Staroverov, R. Kobayashi, J. Normand, K. Raghavachari, A.P. Rendell, J.C. Burant, S.S. Iyengar, J. Tomasi, M. Cossi, N. Rega, N.J. Millam, M. Klene, J.E. Knox, J.B. Cross, V. Bakken, C. Adamo, J. Jaramillo, R. Gomperts, R.E. Stratmann, O. Yazyev, A.J. Austin, R. Cammi, C. Pomelli, J.W. Ochterski, R.L. Martin, K. Morokuma, V.G. Zakrzewski, G.A. Voth, P. Salvador, J.J. Dannenberg, S. Dapprich, A.D. Daniels, Ö. Farkas, J.B. Foresman, J.V. Ortiz, J. Cioslowski, D.J. Fox, Gaussian 09, Gaussian, Inc., Wallingford, CT, USA, 2009.

[49] R.I. Kaiser, S.P. Krishtal, A.M. Mebel, O. Kostko, M. Ahmed, An experimental and theoretical study of the ionization energies of SiC2Hx (x = 0, 1, 2) isomers, Astrophys. J. 761 (2012) 178.

[50] D. Beaudoin, J.D. Wuest, Dimerization of aromatic C-nitroso compounds, Chem. Rev. 116 (2016) 258–286.